

Specific Heats of Some Cubic Superconducting Titanium-Molybdenum Alloys between 1.1 and 4.3°K*

R. R. HAKE

Atomics International, Division of North American Aviation, Inc., Canoga Park, California

(Received May 1, 1961)

The specific heats of four bcc Ti-Mo alloys have been measured between 1.1° and 4.3°K, and at atomic fractional Mo concentrations between 0.0625 and 0.0860 (sufficient to stabilize the bcc phase). The normal state molar specific heats can be represented by the usual expression $C_n = \gamma T + \beta T^3$, where it is commonly assumed that $\gamma \propto N(E_F)$, the energy density of electronic states at the Fermi energy, and $\beta \propto \theta_D^{-3}$. For each of the alloys the apparent electronic superconducting state specific heat for $1.3 < (T_c/T) < 2.6$ can be represented as $C_{es}/\gamma T_c = a \exp(-bT_c/T)$ where $a = 10.5$, $b = 1.52$, and the superconducting transition temperature, T_c , is taken as the midpoint of the rather broad (≈ 0.45 K°) super-

conducting transition. The measured values of T_c , θ_D , and γ are all rapidly varying and nearly linear functions of atomic fractional Mo concentration, f . At the mean solute concentration ($f = 0.0742$): $T_c = 2.59^\circ\text{K}$, $d \ln T_c / df = +16.7$; $\theta_D = 337^\circ\text{K}$, $d \ln \theta_D / df = -6.2$; $\gamma = 5.45$ millijoules/mole (K°)², $d \ln \gamma / df = d \ln N(E_F) / df = +7.7$. On the basis of the Bardeen-Cooper-Schrieffer theory of superconductivity, the relative variations of T_c , θ_D , and $N(E_F)$ indicate that the electron-electron interaction parameter of that theory, A , is a *relatively* slowly varying function of solute concentration ($d \ln A / df = -3.0$).

I. INTRODUCTION

CALORIMETRIC measurements on alloys at liquid helium temperatures are of potential interest from several different standpoints. Accurate measurements as a function of temperature in this region normally allow a separation of the electronic and lattice contributions to the specific heat and yield values for the energy density of electronic states at the Fermi energy, $N(E_F)$, and the limiting low-temperature value of the Debye temperature, θ_D . The magnitude of $N(E_F)$ as a function of alloying may offer information concerning the electronic energy band structure. Aside from obtaining information on band structure *per se*, an understanding of certain fundamental metallic properties may be enhanced by correlating their alloying dependencies with those of $N(E_F)$ and θ_D , since these are important single parameters characterizing the electron and phonon distributions. Then too, specific heat measurements as a function of temperature and alloying may help to elucidate the nature of any special ordering processes, such as superconductivity, which occur in the temperature region of measurement.

The present investigation¹ of helium temperature specific heats of Ti-rich bcc Ti-Mo alloys is of some interest in all of the above respects. Earlier transport property measurements² showed that the electrical resistivities of these alloys are high (≈ 140 $\mu\text{ohm-cm}$ just above the superconducting transition temperatures), that the solute concentration dependence as well as the temperature dependence of the resistivity is unusual, and that the alloys become superconducting at liquid helium temperatures with resistive superconducting transition temperatures increasing rapidly as a function of Mo concentration. The relevance of the

present calorimetric results to the resistive behavior has been previously indicated,^{1,2} and in this paper emphasis will be placed upon the interrelationship of T_c , $N(E_F)$, and the electronic band structure. In addition, the temperature and alloying dependence of the apparent electronic superconducting state specific heat will be discussed.

II. APPARATUS AND EXPERIMENTAL METHOD

A. Method

Fairly standard methods of low-temperature calorimetry^{3,4} were employed in these measurements. The discontinuous heating method was used. An accurately measured small amount of heat was supplied to a thermally isolated specimen coupled to a "core" containing a resistance heater and a temperature-calibrated carbon resistor thermometer. The heat input, ΔQ , divided by the resultant measured temperature rise, ΔT , gave the average heat capacity of the specimen and core over the temperature range ΔT (≈ 0.03 K°). For each alloy specimen about fifty such determinations were made in the temperature region between 1.1° and 4.3°K. The relatively small heat capacity of the core alone was determined in the same manner in a separate experiment. The data reduction was accomplished via an IBM 709 computer.

B. Cryostat

Figure 1 shows a schematic view of the lower portion of the calorimeter cryostat. A 0.17-in. diam hole is drilled through the specimen so that it can be placed over the copper core to which are attached the carbon resistor thermometer and the manganin wire heater coil. The thermometer is a nominal 39-ohm, 1/10-w, Allen-Bradley carbon resistor having a resistance of ≈ 340 ohm at 4.3°K and $\approx 12\,000$ ohm at 1.1°K.

* This research was supported by the U. S. Atomic Energy Commission.

¹ For a brief report of this work see R. R. Hake, *Proceedings of the Seventh International Conference on Low-Temperature Physics, 1960* (University of Toronto Press, Toronto, 1960).

² R. R. Hake, D. H. Leslie, and T. G. Berlincourt, *J. Phys. Chem. Solids* **20** (to be published).

³ P. H. Keesom and N. Pearlman in *Encyclopedia of Physics*, edited by S. Flügge (Springer-Verlag, Berlin, 1956), Vol. XIV, p. 282.

⁴ D. H. Parkinson, *Repts. Progr. Phys.* **21**, 226 (1958).

Adequate thermal contact between the specimen and core is achieved by tightening a copper nut so that the specimen is pressed down firmly against a beryllium-copper spring. The core is suspended inside a brass can by thin nylon threads. Two pairs of spiraled superconducting Nb wire leads (0.002-in. diam) connect the heater and thermometer to lead-through terminals at the bottom of the can. Each pair of Nb leads connects to separate copper current and potential leads in the liquid helium bath. The can may be opened at the soft solder joint and specimens can be easily interchanged without rewiring. Thermal contact between the core-specimen assembly and the liquid helium bath surrounding the can is made and broken by the use of a mechanical heat switch similar to that described by Webb and Wilks.⁵ Using the heat switch, the specimen and core can be cooled from room temperature to the lowest temperature attainable by pumping on the outer liquid helium bath ($\approx 1.1^\circ\text{K}$) without the introduction of any exchange gas. Opening the switch at the lowest temperatures in order to isolate thermally the specimen results in a heat input of about $20\ \mu\text{joules}$, sufficient to raise the temperature of the present specimens only about $0.005\ \text{K}^\circ$. The liquid helium vapor pressure bulb is toroidal and has a total volume of about $20\ \text{cm}^3$. The bulb connects with manometers through a vacuum-jacketed thin-walled stainless steel tube which is thermally connected to the helium bath just above the vapor pressure bulb by means of a copper radiation trap.

C. Measurement of Heat Capacity

1. Heating Curves

After a specimen had been cooled to $\approx 1.1^\circ\text{K}$, the heat switch was opened and measurements of the heat capacity were begun. The measuring current through the carbon resistor thermometer was varied from $0.5\ \mu\text{a}$ at the lowest temperatures to $10\ \mu\text{a}$ at the highest, so that the resultant power dissipation in the thermometer was less than $10^{-8}\ \text{w}$ below 2.5°K and less than $3.7 \times 10^{-8}\ \text{w}$ above 2.5°K . The voltage across the thermometer was balanced against that of a Rubicon six-dial thermofree potentiometer, the off-balance signal being amplified and displayed continuously as a function of time on a fast-response millivolt recorder. Analysis of the off-balance voltage drifts measured during the present experiment showed that the background heat influx with specimen and bath at the same temperature averaged about $3 \times 10^{-8}\ \text{w}$ ($18\ \text{ergs/min}$), after care had been taken to reduce vibration to a minimum. With specimen and bath at different temperatures the thermometer drifts indicated an effective thermal conductance between the two of about $7 \times 10^{-8}\ \text{w/K}^\circ$, being a factor of two higher or lower depending on the temperature of the Nb leads and nylon supports (since their thermal conductivities are temperature dependent).

⁵ F. J. Webb and J. Wilks, Proc. Roy. Soc. (London) A230, 549 (1955).

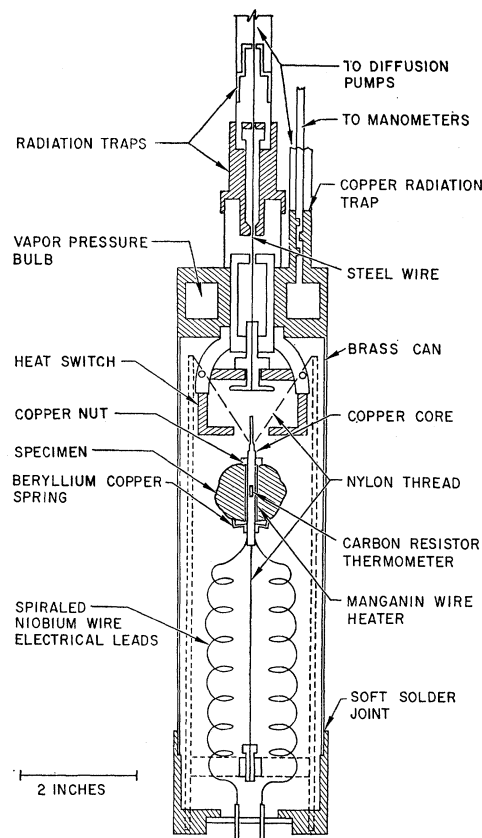


FIG. 1. Schematic view of the lower portion of the calorimeter cryostat.

Figure 2 shows some typical heating curves traced from the recorder chart. The overshoot of the thermometer which is apparent in these traces is evidently due to the low thermal conductivity of the alloy specimens, since no thermometer overshoot was observed during a test run on a pure Cu specimen. Directly after the heat input the off-balance signal was rezeroed so that the amplifier and recorder were used essentially as null indicators. The thermal isolation of the specimen was such that the drifts before and after the heating period were effectively linear. Extrapolation of these drifts to the midpoint of the heating period determined the drift-corrected voltages V_b and V_a across the thermometer (hence, corresponding thermometer resistances R_b and R_a) before and after the heating period. The heat input is calculated from the voltages V_h across the heater coil and V_s across a standard resistor, R_s , in series with the coil; and the heating time, τ , as read to 0.001 sec on a timer (actuated by the same relay which switches the heating current) powered by a 60-cps frequency standard. The heat capacity, C , at $(T_a + T_b)/2$ is then taken as

$$C = \Delta Q / \Delta T = (V_h V_s \tau R_s^{-1}) / (T_a - T_b), \quad (1)$$

where $T_a(R_a)$ and $T_b(R_b)$ are obtained from the thermometer calibration.

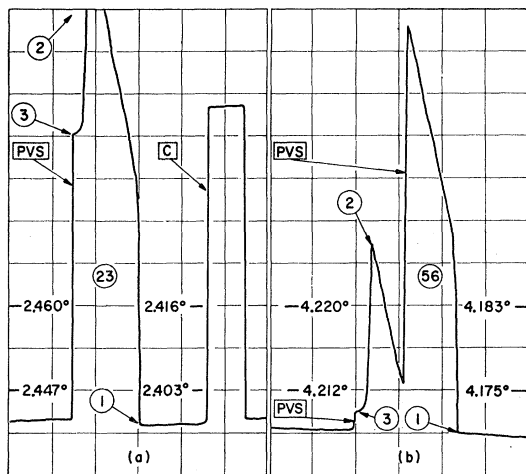


FIG. 2. Typical heating curves (traced from the recorder chart). Time increases from right to left. (a) Ti-0.0650 Mo specimen (0.586 mole) plus core, heat No. 23. Approximate values of pertinent data: outer helium bath temperature, 1.1°K; average specimen temperature, 2.42°K; heating power, 9.33×10^{-6} w; heat input, 3.51×10^{-4} joule; heating period, 37.7 sec; temperature increase of specimen, 0.0434 K°; voltage calibration signal, 42 μ v. (b) Ti-0.0650 Mo specimen plus core, heat No. 56. Approximate values of pertinent data: outer helium bath temperature, 4.2°K; average specimen temperature, 4.19°K; heating power, 9.34×10^{-6} w; heat input, 5.60×10^{-4} joule; heating period, 60 sec; temperature increase of specimen, 0.0373 K°. The notations on the traces have the following meanings: C, voltage calibration signal; PVS, shift of trace via potentiometer voltage shift; 1, heating current switched into heater from standby heater; 2, heating current switched out of heater to standby heater; 3, thermometer, core, and specimen equilibrate.

2. Thermometer Calibration

Upon completion of the heating curve measurements, the carbon resistor thermometer was calibrated against the vapor pressure of liquid helium. Helium exchange gas was admitted to the vacuum chamber surrounding the specimen in order to insure good thermal coupling between specimen, vapor pressure bulb, and liquid helium bath. Calibration points were taken every 0.2 K° between 1.1° and 4.3°K. At each point the temperature of the outer helium bath could usually be held constant to better than 10^{-4} K°/min by the use of a Wallace and Tiernan regulator at high pressures and an electronic heat-pulse regulator⁶ at lower pressures. In order to reduce variable temperature gradients in the helium bath above the λ point, 0.2 w was dissipated in a resistor at the bottom of the helium bath during regulation.⁷ The vapor pressures were measured by means of 22 mm i.d. mercury and oil manometers read to 0.02 mm with a Wild Heerbrugg cathetometer. Above the λ point the vapor pressure of liquid helium in the vapor pressure bulb was measured. Below the λ point the vapor pressure of the outer helium bath was measured, since

thermomolecular pressure differences in the tubes connecting the vapor pressure bulb to the manometers become significant below the λ point,⁸ whereas the need for the hydrostatic head correction in a deep bath of liquid helium disappears. The vapor pressure readings were transcribed directly onto a recorder chart which maintained a continuous record of the off-balance thermometer voltage together with standard voltage reference signals taken from across a decade resistor in series with the thermometer.

The vapor pressure readings were reduced to standard temperature and gravity and converted to temperatures using the 1958 He⁴ Scale.⁹ It was found that these temperatures, T , could be represented as a function of the thermometer resistance, R , to within 0.04 K° at 1.1°K and 0.005 K° at 4.0°K using the two-parameter equation

$$T_r = \log_{10} R / (A \log_{10} R + E)^2, \quad (2)$$

with $A = +0.70832$ and $E = -1.0291$. An error curve, $(T_r - T)$ vs T_r , readable to 10^{-5} K°, was plotted for each calibration series and used along with (2) to determine $T_a(R_a)$ and $T_b(R_b)$ in (1). For five runs made consecutively with the present apparatus (after elimination of a small Nb lead contact resistance) the maximum separation of the five error curves was 0.003 K°, occurring at about 4°K. It is uncertain whether this small shift was due to a change in the resistance of the thermometer or to varying thermal gradients during the calibrations. No discontinuities of more than 0.001 K° in the error curves are evident at the λ point, such as might be expected if thermal gradients were responsible for the calibration shifts.

3. Errors

Each of the quantities on the right of (1) is known to better than 0.1% except $(T_a - T_b)$. Random errors of about 0.3% in $(T_a - T_b)$ may occur due to uncertainties associated with the extrapolation of the temperature drifts to the midpoints of the heating periods. Systematic errors of about 0.5% may arise because of uncertainty in vapor pressure temperature calibration, as discussed recently by Phillips.¹⁰ It is estimated that all other possible sources of systematic error (including that due to uncertainty in the value of the core heat capacity) result in a total possible systematic error in each heat capacity determination of $\pm 1\%$. A determination of the specific heat of pure copper using the present apparatus yielded $\gamma = 0.700 \pm 0.003$ mJoule/mole (K°)² and $\theta_D = 345.6 \pm 0.7^\circ$ K, where the errors are probable errors as calculated by the method of least squares.¹¹ The estimated systematic error is $\pm 1\%$ in both γ and

⁸ T. R. Roberts and S. G. Sydorik, Phys. Rev. **102**, 304 (1956).

⁹ F. G. Brickwedde, H. van Dijk, M. Durieux, J. R. Clement, and J. K. Logan, J. Research Natl. Bur. Standards **64A**, 1 (1960).

¹⁰ N. E. Phillips, Phys. Rev. **114**, 676 (1959).

¹¹ See for example H. Margenau and G. M. Murphy, *The Mathematics of Physics and Chemistry* (D. Van Nostrand Company, Inc., Princeton, 1943), p. 502.

⁶ R. R. Hake and D. E. Mapother, J. Phys. Chem. Solids **1**, 199 (1956).

⁷ F. E. Hoare and J. E. Zimmerman, Rev. Sci. Instr. **30**, 184 (1959).

θ_D . These values agree within the combined systematic plus random error limits with those quoted by Rayne¹² from his own work¹³ and that of Corak *et al.*¹⁴ of $\gamma = 0.687 \pm 0.012$ mJoule/mole $(K^\circ)^2$ and $\theta_D = 344.5 \pm 3^\circ K$, where the errors are the random errors plus an estimated $\pm 0.5\%$ systematic error.

D. Heat Capacity of the Core

The heat capacity of the core alone was measured in a separate run. The total weight of the copper core with carbon resistor and manganin wire heater coil was 5.38 g. The measured heat capacity of the core could be represented between 1.1 and $5^\circ K$ as

$$C_c(T) = (0.0573 \pm 0.0013)T + (0.00562 \pm 0.00009)T^3, \quad (3)$$

where $C_c(T)$ is in mJoules/ K° . The error limits are the probable errors as calculated by the method of least squares. For the alloy specimens measured in this experiment the core constituted a maximum of 4.3% of the total heat capacity [for the Ti-0.0625 Mo specimen (i.e., f = atomic fractional Mo concentration = 0.0625) at $4.3^\circ K$].

E. Specimens

Relevant metallurgical considerations regarding bcc Ti-Mo alloys and their preparation have been previously summarized,² and only brief mention of such information will be made here. The bcc phase of pure Ti is stable from the melting point down to about $1156^\circ K$, at which point it transforms martensitically to the low temperature stable hcp phase. Addition of Mo to Ti lowers the bcc to hcp transformation temperature, and above these temperatures there is complete solid solubility of Mo in bcc Ti. Microscopic examinations of Ti-Mo alloys which have been quenched from the region of solid solubility to room temperature indicate complete bcc phase retention in alloys with atomic fractional Mo concentrations, f , such that $f \geq \approx 0.05$ according to Hansen *et al.*,¹⁵ or $f \geq 0.058 - 0.068$ according to Duwez.¹⁶

Weighed amounts of Foote Mineral Company crystal-bar, iodide-process Ti of nominal purity 99.92% and A. D. MacKay, Inc. Mo of nominal purity 99.9% were melted together in a laboratory arc furnace utilizing a "gettered" argon atmosphere, a water-cooled copper hearth, and a tungsten electrode. Each of the alloys was turned over and remelted at least six times to promote homogeneity. Weight loss of the calorimetric specimens was in each case less than 0.035% so that alloy composition could be adequately determined from

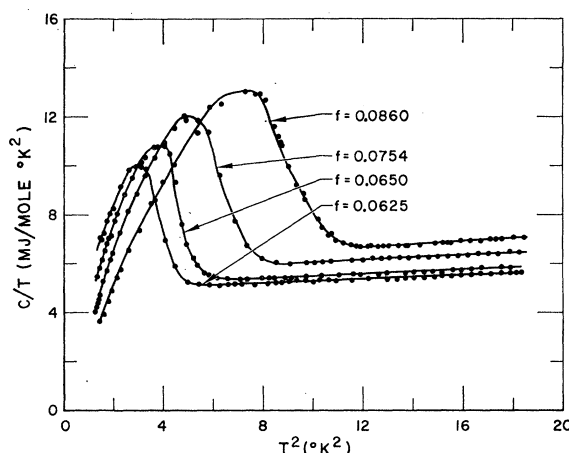


FIG. 3. C/T vs T^2 for different atomic fractional concentrations, f , of Mo.

the weights of the starting materials. Upon breaking the arc a rapid quenching of the melt, in contact with the water-cooled copper hearth, occurred. The arc-melted buttons (about 32 g each) were measured calorimetrically in the as-cast condition (the only fabrication was the drilling of a 0.17-in. hole through the centers of the buttons for the accommodation of the core). Since Ti is extremely reactive, it was felt that the risks of contaminating the specimens during the cold working and the lengthy high temperature annealing required to improve the alloy homogeneity outweighed the danger that the calorimetric results might be seriously influenced by the coring which is commonly observed in as-cast Ti-Mo arc-melted buttons. Previous work² showed that the removal of all microscopic evidence of such coring from one bcc Ti-Mo alloy strip (by severe cold working and subsequent vacuum annealing at $1000^\circ C$ for 9 hr) caused no significant departures from the usual resistivity, Hall effect, or resistive superconducting behavior observed in specimens cut from the as-cast arc-melted buttons. The widths of the calorimetrically measured superconducting transitions ($\Delta T \approx 0.45 K^\circ$, see Table II and Fig. 3) together with the measured solute concentration dependence of T_c ($dT_c/df = 43$, from Fig. 4) suggest a total spread in solute concentration over the cored regions in each of the buttons of no more than about ± 0.5 atomic percent. The macroscopic inhomogeneity could be less than this if, as seems likely, the transition breadths are determined primarily by "statistical inhomogeneity" (see Sec. III-A), and/or if strains contribute to the transition broadening.

X-ray, micrographic, electrical resistivity, and hardness examinations in this laboratory² on sections cut from the inner portions of as-cast arc-melted buttons have always indicated complete bcc phase retention (with no indication of ω phase) for Ti-Mo alloys arc-melted as described above with $0.0708 \leq f \leq 0.2327$. X-ray lattice parameter determinations (solid surface

¹² J. A. Rayne, Phys. Rev. **110**, 606 (1958).

¹³ J. A. Rayne, Australian J. Phys. **9**, 189 (1956).

¹⁴ W. S. Corak, M. P. Garfunkel, C. B. Satterthwaite, and A. Wexler, Phys. Rev. **98**, 1699 (1955).

¹⁵ M. Hansen, E. L. Kamen, H. D. Kessler, and D. J. McPherson, Trans. AIME **191**, 881 (1951).

¹⁶ P. Duwez, Trans. AIME **191**, 765 (1951).

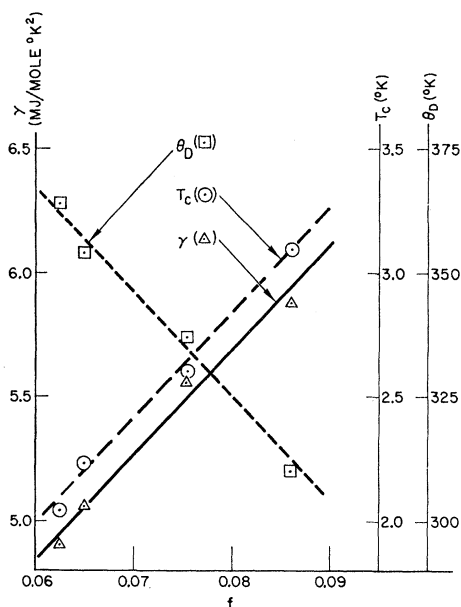


FIG. 4. γ , T_c , and θ_D vs atomic fractional concentration, f , of Mo.

back reflection data taken with a Norelco diffractometer, spinning specimen) on such alloys are in reasonable agreement with the results of Hansen *et al.*¹⁵ Resistivity measurements between 1.1° and 300°K on such specimens have given no indication of a crystallographic phase transformation below room temperature.²

Because the calorimetric specimens were prepared in an identical manner and from the same starting materials as reported in the earlier transport property work,² it was not considered necessary to subject the higher Mo concentration specimens to the usual x-ray, micrographic, resistivity, and hardness tests. However, upon completion of the specific heat measurements, the calorimetric specimen with the lowest Mo concentration (Ti-0.0625 Mo) was cut into sections and examined. Microscopic and x-ray observations on four different surfaces exposed by cutting through the button near the center, where the quenching time was probably longest, indicated that the button was entirely bcc with a lattice parameter of 3.265 ± 0.005 Å as expected for Ti-0.0625 Mo from previous x-ray work.² The microscopic observations also disclosed the usual degree of coring. Since no hcp material was seen, it is evident that the Mo-lean regions must contain at least 5–6 atomic percent Mo.^{15,16} The average of twelve hardness readings taken over two of the four surfaces was DPH 250 (range 245–255), showing that the presence of ω phase in this specimen was unlikely.

The results of resistivity and Hall coefficient measurements on two sections cut from the calorimetrically measured Ti-0.0625 Mo specimen are listed in Table I. The data for the two specimens are nearly the same and are in excellent agreement at all temperatures with

extrapolations to $f=0.0625$ of previous resistivity and Hall coefficient data for bcc Ti-Mo alloys with $0.0708 \leq f \leq 0.2327$.² As in previous work, the Hall coefficients were magnetic field independent up to the highest measuring fields (30 kgauss). The resistive superconducting transitions of the two specimens were also nearly identical (at equal measuring current densities) and similar in shape to those measured earlier in other bcc Ti-Mo samples.² At measuring current densities on the order of 60 amp/cm², the extrapolations of the steep linear portions of the ρ vs T curves intersected the $\rho=0$ axes at 1.7°K, a temperature close to the maximum of the Ti-0.0625 Mo specimen specific heat vs T curve (similar in shape to the curves shown in Fig. 3).

III. EXPERIMENTAL RESULTS

A. Superconducting Transitions

Figure 3 shows C/T vs T^2 plotted for the four bcc Ti-Mo alloys of different atomic fractional Mo concentrations. The negative slope portions of the curves are due to the superconducting transitions. The relative position of the peaks shows that the superconducting transition temperature, T_c , increases rapidly as Mo concentration is increased, in agreement with earlier resistive determinations.² For each of the alloys, T_c has been taken as the midpoint temperature of the rather broad ($\Delta T \approx 0.45$ K°) negative slope transition region. The T_c values are listed in Table II and plotted as a function of Mo concentration in Fig. 4. At the mean solute concentration, $f=0.0742$:

$$T_c = 2.59^\circ\text{K}, \quad d \ln T_c / df = +16.7, \quad (4)$$

(i.e., a 16.7% increase in T_c per atomic percent increase in Mo). Similar sensitivity of T_c to alloying addition has been observed by Matthias^{17,18} in other transition metal alloy systems. The present observed increase in T_c with solute concentration is consistent with the Matthias regularities¹⁷ in that as Mo is added to Ti the average number of "valence" electrons per atom

TABLE I. Results of electrical resistivity (ρ) and Hall coefficient (R) measurements on two specimens, Q1 and Q2, cut from the left and right sides, respectively, of the middle portion of the bcc Ti-0.0625 Mo calorimetric specimen after completion of the specific heat measurements.

T (°K)	ρ ($\mu\text{ohm-cm}$)		R (10^{-5} cm ³ /Coulomb)	
	Q1	Q2	Q1	Q2
≈ 293	149.0	148.9	+22.4	+22.1
273	149.5	149.0
195	149.6	149.3
77	148.1	147.8	+39.8	+39.5
4.2	147.9	147.7	+43.3	+43.7

¹⁷ B. T. Matthias in *Progress in Low-Temperature Physics*, edited by C. J. Gorter (Interscience Publishers, Inc., New York, 1957), Vol. II, p. 138.

¹⁸ B. T. Matthias, V. B. Compton, H. Suhl, and E. Corenzwit, *Phys. Rev.* **115**, 1597 (1959).

TABLE II. Specific heat results for bcc Ti-Mo alloys.

f^a	γ^b	θ_D (°K) ^c	T_c (°K) ^d	r (%) ^e	ΔT (K°) ^f	p_n^g
0.0625	4.90±0.014	364±3.3	2.04	0.46	0.41	34
0.0650	5.06±0.013	354±2.7	2.23	0.25	0.39	22
0.0754	5.56±0.014	337±1.9	2.60	0.29	0.50	29
0.0860	5.88±0.019	310±2.0	3.09	0.14	0.53	21

^a Atomic fractional Mo concentration.^b Electronic specific heat coefficient in units of millijoules/mole (K°)². Only the probable error is indicated. Estimated systematic error is ±1%.^c Debye temperature. Only the probable error is indicated. Estimated systematic error is ±3%.^d Superconducting transition temperature (transition midpoint).^e Average percentage residual of normal state data points (C/T) from linear least-squares fit of C/T to T^2 .^f Superconducting transition breadth (as defined in the text).^g Number of data points taken in the normal state.

moves closer to 5. Matthias *et al.*¹⁸ have recently observed that addition of Cr, Mn, Fe, or Co to bcc Ti produces increasing transition temperatures up to average valence electron per atom concentrations of 4.4 to 4.7.

Inhomogeneity appears to be the most likely cause of the relatively broad zero-field superconducting transitions often observed in superconducting alloys. It is uncertain that this inhomogeneity need be of a macroscopic type, for it can be argued¹⁹ that even in perfectly random solid solution alloys, statistical fluctuations in composition over domains of size comparable to the superconducting electronic "coherence distance,"²⁰ ξ , could result in considerable broadening of the superconducting transition if ξ is short and T_c is a strongly varying function of composition. In the case of the present high-resistivity alloys the electronic mean free path, and therefore ξ , should be relatively small. This small ξ , together with the observed high value of dT_c/df , suggests that statistical "inhomogeneity" could be primarily responsible for the broad transitions, although macroscopic inhomogeneity (some degree of coring has been observed in similarly made alloys²) and strains also probably play a role. It can be shown that Gaussian compositional distributions appropriate to $\xi \approx 70$ Å would result in transition shapes similar to those observed (Fig. 3), but would not significantly alter the net electronic specific heat in the normal or superconducting states from that which would be observed if every domain of dimension ξ had the average or nominal composition of the alloy.²¹ The small range of coherence in these alloys might also help to account²⁰ for their

proclivity to display zero resistance in the presence of magnetic fields of 20–30 kgauss.²

B. Normal State

In the normal state above the peaks due to the superconducting transitions the C/T vs T^2 curves are linear indicating that the usual relationship

$$C_n(T) = \gamma T + \beta T^3, \quad (5)$$

is obeyed by these alloys. Here γT and βT^3 are normally identified as, respectively, the electronic and lattice contribution to the specific heat. For each of the alloys the data in the linear C/T vs T^2 region were used to obtain values of γ and β and their probable errors by the method of least squares.¹¹ The scatter of the individual data points from the least squares fits appeared to be random. For each alloy the average percentage residual, r , is listed in Table II, along with the value of γ and the value of θ_D as calculated from the relationship³

$$\theta_D = (1.944/\beta)^{1/3} \times 10^2 \text{ °K}, \quad (6)$$

where β is in mJoules/mole (K°)⁴. The probable errors in γ and θ_D indicated in Table II include those of the core heat capacity (3). The estimated systematic errors are ±1% for γ and ±3% for θ_D . The values of γ and θ_D are plotted as functions of the atomic fractional Mo concentration in Fig. 4. The solute concentration dependence of both γ and θ_D is surprisingly high. At the mean solute concentration, $f=0.0742$:

$$\gamma = 5.45 \text{ mJoules/mole (K°)}^2, \quad d \ln \gamma / df = +7.7, \quad (7)$$

$$\theta_D = 337 \text{ °K}, \quad d \ln \theta_D / df = -6.2. \quad (8)$$

If, as is normally assumed, $\gamma \propto N(E_F)$, then from (7)

$$d \ln N(E_F) / df = +7.7. \quad (9)$$

C. Superconducting State

For each of the alloys the electronic contribution, C_{es} , to the superconducting state specific heat was separated from the total superconducting state specific heat, C_s , by assuming that the lattice contribution to C_s was βT^3 , where β was determined in the normal state above the zero-field superconducting transitions:

$$C_{es}(T) = C_s(T) - \beta T^3. \quad (10)$$

The value of βT^3 is at most 3% of C_s (for the case of Ti-0.0625 Mo at 1.1°K). Thus the uncertainty in C_{es} due to the possibility that (a) the value of β might be slightly temperature dependent below 4°K (this would not be expected since the lowest θ_D is 310°K), or (b) the value of β might be different in the normal and superconducting states^{22,23} (but see reference 24), is expected

²² C. A. Bryant and P. H. Keesom, Phys. Rev. Letters 4, 460 (1960).

²³ H. A. Boorse, A. T. Hirshfeld, and H. Leupold, Phys. Rev. Letters 5, 246 (1960).

²⁴ B. S. Chandrasekhar and J. A. Rayne, Phys. Rev. Letters 6, 3 (1961).

¹⁹ A. Calverley and A. C. Rose-Innes, Proc. Roy. Soc. (London) A255, 267 (1960).

²⁰ T. E. Faber and A. B. Pippard in *Progress in Low Temperature Physics*, edited by C. J. Gorter (Interscience Publishers, Inc., New York, 1955), Vol. I, p. 159.

²¹ In the pertinent calculations it is assumed that (a) a domain of average atomic fractional solute concentration, f_d , undergoes a discontinuous superconducting transition at a T_c determined by f_d in accordance with Fig. 4, (b) a domain has electronic specific heats of the form indicated in (5) and (11) where γ and T_c are determined by f_d in accordance with Fig. 4, and (c) that the electronic specific heat of the alloy is determined by the sum of independent contributions from the individual domains.

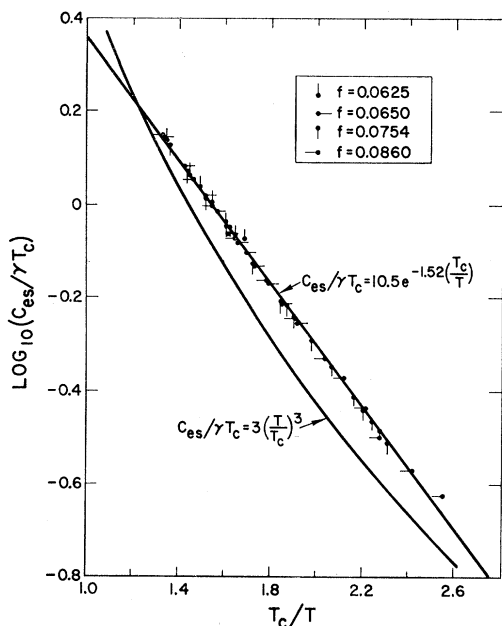


FIG. 5. The reduced superconducting state electronic specific heat, $C_{es}/\gamma T_c$, vs T_c/T for different atomic fractional concentrations, f , of Mo. For comparison the once accepted relationship $C_{es}/\gamma T_c = 3(T/T_c)^3$ is also shown.

to be small. In Fig. 5, $\log_{10}(C_{es}/\gamma T_c)$ is plotted as a function of reduced temperature, T_c/T . For comparison, a curve describing the once accepted relationship $C_{es}/\gamma T_c = 3(T/T_c)^3$ is also shown. The linearity of the curve describing the data points indicates that for each of the alloys the apparent C_{es} is exponential in $(1/T)$ to within experimental error, as has been found to be the case for many pure element superconductors in this same range of reduced temperature, $1.3 < (T_c/T) < 2.6$.²⁵ The apparent superconducting state electronic specific heats for these alloys obey a law of corresponding states such that

$$C_{es}/\gamma T_c = a \exp(-bT_c/T), \quad (11)$$

with $a=10.5$ and $b=1.52$. These a and b values are close to those observed for the superconductors Sn, V, Ta, and Nb in the same range of reduced temperature.²⁵ According to the BCS theory of superconductivity²⁶ (11) is approximately valid in the region $2.5 \leq (T_c/T) \leq 6$ with $a=8.5$ and $b=1.44$.²⁷

The apparent a and b values as obtained graphically (Fig. 5) depend upon the choice of T_c , and it can be seen from (11) that a $\pm\epsilon\%$ change in the T_c value used in plotting the data as in Fig. 5 will result in a $\mp\epsilon\%$ change in the apparent values of a and b . The T_c values listed in Table II and used in Fig. 5 were obtained from

²⁵ For a review see M. A. Biondi, A. T. Forrester, M. P. Garfunkel, and C. B. Satterthwaite, *Revs. Modern Phys.* **30**, 1109 (1958).

²⁶ J. Bardeen, L. N. Cooper, and J. R. Schrieffer, *Phys. Rev.* **108**, 1175 (1957).

²⁷ J. Bardeen and J. R. Schrieffer (to be published).

large scale plots of C vs T , T_c being taken as $(T_{\max} + T_{\min})/2$ where T_{\max} and T_{\min} are, respectively, the temperatures at the maximum and minimum heat capacities on the low and high temperature sides of the transitions. It is believed that any other reasonable convention for picking the transition midpoints would result in T_c values at most ± 0.01 K° different from those listed in Table I. Thus the uncertainty in a and b values due to the arbitrariness of choosing T_c ranges from $\pm 5\%$ for the Ti-0.0625 Mo specimen to $\pm 3\%$ for the Ti-0.0860 Mo specimen. The transition breadths, ΔT , defined as $(T_{\max} - T_{\min})$ are listed in Table II. That it should be the transition midpoint which is used for T_c in calculating values of a and b appears reasonable considering that the observed specific heat in the superconducting state is probably not significantly different from that which would be observed in a strictly "homogeneous" alloy of the same nominal composition (Sec. III A). Such an ideal alloy would have a T_c very close to the observed superconducting transition midpoint of the actual alloy.

IV. DISCUSSION

A. Solute Concentration Dependence of T_c

An interesting feature of the present results is the rapid increase in both the electronic specific heat coefficient, γ , and the superconducting transition temperature, T_c , as Mo concentration is increased. According to the Bardeen-Cooper-Schrieffer (BCS) theory of superconductivity²⁶

$$kT_c = 1.14 \langle \hbar \omega \rangle_{\text{av}} \exp\{-V_m/[N(E_F)A]\}, \quad (12)$$

or, approximately, following Morel,²⁸

$$T_c = 0.85 \theta_D \exp\{-V_m/[N(E_F)A]\}. \quad (13)$$

Here $N(E_F)$ is the normal state energy density of electronic states at the Fermi level for one spin direction per mole, V_m is the molar volume, and A is the electron-electron interaction parameter of the theory. Differentiating (13) with respect to solute concentration, f :

$$\begin{aligned} d \ln T_c / df = & d \ln \theta_D / df + [\ln(0.85 \theta_D / T_c)] \\ & \times [d \ln A / df + d \ln N(E_F) / df - 3 d \ln p / df], \end{aligned} \quad (14)$$

where p is the lattice parameter ($p^3 \propto V_m$). X-ray measurements in this laboratory² indicate

$$d \ln p / df = -0.064, \quad (15)$$

at the mean concentration of Mo for the present alloys, $f=0.0742$. Inserting into (14) this value and values for the other quantities appropriate to $f=0.0742$ from (4), (8), and (9), we obtain

$$d \ln A / df = -3.0. \quad (16)$$

Thus if the calorimetric data are analyzed within the framework of the BCS theory, they indicate that the

²⁸ P. Morel, *J. Phys. Chem. Solids* **10**, 277 (1959).

electron-electron interaction parameter of that theory is, in the present case, a *relatively* slowly varying function of solute concentration. Goodman *et al.*²⁹ have deduced that A is not appreciably dependent upon solute concentration in the case of superconducting bcc U-Mo alloys via a similar analysis of their calorimetric results.

In order to explain the Matthias regularities for transition metals and alloys on the basis of the BCS theory, Pines³⁰ has suggested that in these metals A and $N(E_F)$ are to a large extent decoupled and that A is much the same for all of them. The observation of maxima in T_c at $n \approx 3, 5, 7$ for transition metals and alloys [n is the average number per atom of "valence" electrons (i.e., electrons outside closed shells in the free atom)] might then be attributed, according to (12), to similar maxima in $N(E_F)$ as a function of n . $N(E_F)$ as obtained from electronic specific heat measurements on pure transition metals in the 4th, 5th, and 6th periods does show (qualitatively speaking) such maxima when plotted versus n .⁴ That $N(E_F)$ for the alloys studied by Matthias should vary in approximately the same manner with n , regardless of the crystal structure is a matter of some conjecture however. Direct calorimetric measurements on series of superconducting alloys appear to offer a good means of studying the Matthias regularities (or any unusual alloying dependence of T_c ^{18,31}) in the light of the BCS theory, since such measurements provide values not only for T_c but also for $N(E_F)$ and θ_D . Although the present results are in substantial accord with Pines' suggestion, more data of this type over wide concentration ranges in different alloy systems are required before meaningful generalization can be made.

B. Band Structure

If Pines' interpretation is accepted, then it would appear that the T_c vs n regularities observed by Matthias imply the existence of a similar d band for all the transition metals [it is assumed that contributions to $N(E_F)$ from other bands are small], the only effect of alloying them together being to change the position of the Fermi level in this band in accordance with the change in the valence electron concentration. The recent electronic specific heat results of Cheng *et al.*³² on various bcc 3d transition metals and alloys are at least not in marked disagreement with a rigid-band model, and show peaks in the apparent $N(E_F)$ vs n curve at $n \approx 4.5$ –5 and $n \approx 6$ –6.5. The present results ($4.125 \leq n \leq 4.172$) lend some added support to the existence of a peak beyond

$n=4$. If it is assumed that a rigid-band model applies in the present case, that each Mo atom contributes two excess electrons to the conduction band, and that the Sommerfeld relationship,

$$\gamma = \frac{2}{3} \pi^2 k^2 N(E_F), \quad (17)$$

is valid, then it can be shown that the observed linear dependence of γ on f implies that near the Fermi levels of the present alloys

$$N(E) = F \exp(GE), \quad (18)$$

with $G = d \ln N(E)/dE = +8.9(\text{ev})^{-1}$, where $N(E)$ is the energy density of electronic states for one spin direction as in (17).³³ Due to the various assumptions and approximations, (18) can be considered as only suggestive. For comparison, a similar analysis of the nearly linear γ vs f relationship observed by Hoare and Yates³⁴ for Pd-rich Pd-Ag alloys yields (18) with $G = -6.9(\text{ev})^{-1}$. Even more energy-dependent $N(E)$ functions near $n=6$ are suggested by the work of Cheng, Wei, and Beck.³²

It has been suggested that apparent γ values may not be simply related to $N(E_F)$ as in (17) because of heat capacity contributions linear in T which are associated with lattice vibrational or magnetic effects. Jones³⁵ has shown that lattice-electron interactions may give rise to such a term due to the effect of thermal excitation of the conduction electrons on the elastic shear constants and thus on the zero-point lattice vibrational energy. This effect is expected to be large when the Fermi surface touches a zone boundary. Marshall³⁶ has discussed another such linear-in- T contribution to the heat capacity which may occur due to the alignment of the moments of paramagnetic ions in dilute metallic solution. In the present case, it seems unlikely that either

³³ Equation (18) is obtained via integration of the relation $2NdE = dn = zd f = zdN/[0.212(d\gamma/df)]$, where N is the number of electronic states of one spin direction at the Fermi level per (ev) (atom), n is the valence electron concentration per atom, z is the excess valence of the solute, f is the atomic fractional solute concentration, and γ is the electronic specific heat coefficient in millijoules/mole (K^2) so that from Eq. (17) $N = 0.212\gamma$. Taking $d\gamma/df$ to be constant (see Fig. 4), the integration yields Eq. (18) with $G = 0.424 (d\gamma/df)/z = (0.424)(42)/2 = 8.9 (\text{ev})^{-1}$. F in Eq. (18) is 1.05 states of one spin direction/(ev) (atom) if the zero of energy, E , is taken at the Fermi level of the Ti-0.0625 Mo specimen. In this derivation $d\gamma/df$ is assumed to be due entirely to the change in the valence electron concentration in a completely rigid band and lattice expansion due to alloying is not taken into account. Taking γ to be a function of n and V_m , the molar volume, the contribution to $d\gamma/df$ from lattice expansion is $s = (\partial\gamma/\partial V_m)_n (dV_m/df) = (\partial \ln\gamma/\partial \ln V_m)_n \gamma 3(d \ln p/df)$, where p is the lattice parameter. Using Eq. (15), $s = -0.70$ at $f = 0.0742$ if $(\partial \ln\gamma/\partial \ln V_m)_n$ has the free electron gas value of $\frac{2}{3}$; and Eq. (18) still holds to a good approximation with $G = +9.0$. If $(\partial \ln\gamma/\partial \ln V_m)_n = +4$ as indicated for Ta by measurements of the pressure dependence of the superconducting critical field [see C. A. Swenson and C. H. Hinrichs, *Proceedings of the Seventh International Conference on Low-Temperature Physics, 1960* (University of Toronto Press, Toronto, 1960), and J. L. Olsen and H. Rohrer, *Helv. Phys. Acta* **33**, 872 (1960)], then $s = -4.2$ at $f = 0.0742$ and Eq. (18) still holds to a good approximation with $G = +9.8$.

³⁴ F. E. Hoare and B. Yates, *Proc. Roy. Soc. (London)* **A240**, 42 (1957).

³⁵ H. Jones, *Proc. Roy. Soc. (London)* **A240**, 321 (1957).

³⁶ W. Marshall, *Phys. Rev.* **118**, 1519 (1960).

²⁹ B. B. Goodman, J. Hillairet, J. J. Veyssié, and L. Weil, *Proceedings of the Seventh International Conference on Low-Temperature Physics, 1960* (University of Toronto Press, Toronto, 1960).

³⁰ D. Pines, *Phys. Rev.* **109**, 280 (1958).

³¹ B. T. Matthias, M. Peter, H. J. Williams, A. M. Clogston, E. Corenzwit, and R. C. Sherwood, *Phys. Rev. Letters* **5**, 542 (1960).

³² C. H. Cheng, C. T. Wei, and P. A. Beck, *Phys. Rev.* **120**, 426 (1960).

of these effects could be important since this would most likely produce divergence from the observed cubic plus exponential temperature dependence of the specific heat in the superconducting state.

C. Superconducting State Electronic Specific Heat

Although the breadths of the superconducting transitions observed in these alloys cause a degree of uncertainty in the interpretation of the observed superconducting state specific heat, the close agreement of the data for all the alloys (Fig. 5) strongly suggests that the reduced superconducting state electronic specific heat, $C_{es}/\gamma T_c$, is very similar in its magnitude and exponential temperature dependence to that observed in several pure element superconductors in the same range of reduced temperature ($1.3 < T_c/T < 2.6$). According to both theory²⁶ and experiment^{25,37} the electronic energy gap in superconductors is appreciably temperature dependent for $(T_c/T) \lesssim 2.5$. Since the electronic specific heat is directly related to the gap width, the present results could be taken to indicate that these high-resistivity alloys have a temperature-dependent gap rather similar to that of many pure-element superconductors. This is in accord with the ideas of Anderson³⁸ who has suggested that even very intense electronic scattering in "dirty" superconductors

should not cause departure from the usual energy-gap type behavior. At present detailed comparisons of C_{es} with theory are most profitable at higher values of T_c/T than those achieved here, where the gap width is expected to be constant. In this region results on several pure-element superconductors indicate deviations of $C_{es}(T)$ from the BCS expression^{39,40} and in some cases these have been attributed to anisotropy of the energy gap. According to Anderson³⁸ no such anisotropy should be expected in high-resistivity alloys, and thus measurement of their superconducting state electronic specific heats to high values of T_c/T might offer a better test of the predictions of the isotropic-gap BCS theory than do measurements on pure-element superconductors.

ACKNOWLEDGMENTS

I wish to thank S. A. Friedberg, P. H. Keesom, D. E. Mapother, and J. A. Rayne for valuable discussions of calorimetric technique at the inception of this work. The able assistance of D. M. Sellman in the construction of the cryogenic apparatus, of D. H. Leslie in the preparation of specimens, and of C. G. Rhodes and P. C. Romo in performing the micrographic, hardness, and x-ray examinations is gratefully acknowledged. In addition, I am indebted to G. W. Lehman for instruction in computer programming.

³⁹ For a review of calorimetric results see H. A. Boorse, Phys. Rev. Letters **2**, 391 (1959).

⁴⁰ D. K. Finnemore, D. E. Mapother, and R. W. Shaw, Phys. Rev. **118**, 127 (1960).

³⁷ P. L. Richards and M. Tinkham, Phys. Rev. **119**, 575 (1960).

³⁸ P. W. Anderson, J. Phys. Chem. Solids **11**, 26 (1959).